

# Appraising timing response of paleoenvironmental proxies to the Bond cycle in the western Mediterranean over the last 20 kyr

Marta Rodrigo-Gámiz<sup>1,2</sup>  · Francisca Martínez-Ruiz<sup>1</sup> · Francisco J. Rodríguez-Tovar<sup>3</sup> · Eulogio Pardo-Igúzquiza<sup>4</sup> · Miguel Ortega-Huertas<sup>2</sup>

Received: 16 December 2016 / Accepted: 28 June 2017 / Published online: 5 July 2017  
© Springer-Verlag GmbH Germany 2017

**Abstract** The timing of climate responses to the Bond cycle is investigated in the western Mediterranean. Periodicities had been previously reported in a marine sediment record from this region spanning the last 20 kyr, and registered by diverse paleoenvironmental proxies, in particular those associated with terrigenous input, redox conditions, productivity, sea surface temperature (SST) and salinity. Further cross-spectral analyses on these time series reveal leads–lags in the 1400 year climate cycle. Considering as reference a terrigenous input proxy (the K/Al ratio), all the paleoenvironmental proxies displayed time shifts varying from ca. 700 year to ca. 350 year. SST and salinity variations show a first leaded response with the inflow of cold and less salty Atlantic waters. Followed by a time lead of 525 year, progressively arid conditions with an increase of eolian dust transport to the area, given by the Zr/Al signal, are observed. The intensification of dust transport could have triggered a latest biological response, lead by

350 year, with an increase of productivity, as suggested by the Ba/Al ratio. Lastly changes in the Mediterranean thermohaline circulation, indicated by a selected redox proxy (the U/Th ratio), are observed. These results support that the oceanic response triggered the atmospheric response to the Bond cycle in the western Mediterranean. Changes in the North Atlantic Oscillation mode and in the Inter-Tropical Convergence Zone migrations with variations in the monsoon activity or Saharan winds system, are considered as main forcing mechanisms, with a complex relationship of the involved phenomena.

**Keywords** Cross-spectral · Bond cycle · Western Mediterranean · Marine record · Paleoenvironmental proxies

## 1 Introduction

A comparison of climate records, especially at the millennial-time scale and between the northern and southern hemispheres, has allowed to document an asynchronous phase response to climate variability known as climate seesaw (Steig and Alley 2002; Denton and Broecker 2008). Study of the out of phase response (lead–lag) between paleoclimate records at different latitudes underlines the complexity between climate forcings and the responses of the climate system (Broecker 1997; Alley et al. 2002). Climate variability has been related to different forcing mechanisms—including external solar cycles, volcanic forcing, melting of large amounts of icebergs and sea ice and solar irradiance changes—resulting in ocean and atmospheric circulation changes that determine millennial-scale cycles. The three most widely recognized periodicities are those at approximately 2800–2000 year, 1500 and 1000 year (see

**Electronic supplementary material** The online version of this article (doi:10.1007/s00382-017-3782-y) contains supplementary material, which is available to authorized users.

✉ Marta Rodrigo-Gámiz  
martarodrigo@ugr.es

- <sup>1</sup> Instituto Andaluz de Ciencias de la Tierra (IACT), Consejo Superior de Investigaciones Científicas-Universidad de Granada (CSIC-UGR), Avda. de las Palmeras 4, 18100 Armilla, Granada, Spain
- <sup>2</sup> Departamento de Mineralogía y Petrología, Universidad de Granada, Campus Fuentenueva s/n, 18002 Granada, Spain
- <sup>3</sup> Departamento de Estratigrafía y Paleontología, Universidad de Granada, Campus Fuentenueva s/n, 18002 Granada, Spain
- <sup>4</sup> Instituto Geológico y Minero de España (IGME), Madrid, Spain

Smith et al. 2016 and references therein). Yet although multi-decadal to multi-century time scale Holocene cold events are well-known, the mechanisms determining these changes are still under debate (see Wanner et al. 2015 for a recent review). One of the most controversial climate variations is that associated with the so-called Bond cycles (Bond et al. 1993, 1997, 2001; Broecker 1994). Originally a comparison between Greenland oxygen isotope records and North Atlantic sea surface temperature records showed a series of rapid warm-cold oscillations—called Dansgaard-Oeschger events—for the last 90 kyr (Bond et al. 1993). These cycles, lasting on average 10–15 kyr, culminated in a southerly transport of ice-rafting debris (IRD) in the North Atlantic (a Heinrich event) before an abrupt shift to a warmer condition (Bond et al. 1993, 1997, 2001; Smith et al. 2016). Moreover, these cycles documented a previously unrecognized link between ice sheet behaviour and ocean–atmosphere temperature changes.

These cold episodes paced at about the same time during the last glaciation and the Holocene with a cyclicity close to  $1470 \pm 500$  years, although operated independently of the glacial-interglacial climate state (Bond et al. 1997). An important question that remains to be resolved is whether the cycles are driven by external factors, such as orbital forcing, or by internal ice-sheet dynamics. Bond et al. (2001) argued that a solar forcing mechanism could have forced these millennial-scale Bond events at least during the Holocene.

The Bond cycle has been described as quasi-periodic slowdowns of North Atlantic Deep Water (NADW) production feeding into the Atlantic Meridional Overturning Circulation (AMOC), and ensuing cold climate in Europe at the millennial-time scale (Bond et al. 1993, 2001; Broecker 1994). This cycle has been persistently detected in the North Atlantic and Mediterranean climate regions (Bond et al. 1993; Moreno et al. 2005; Debret et al. 2007; Pena et al. 2010; Rodrigo-Gámiz et al. 2014a) related to solar activity and oceanographic circulation. Furthermore, atmospheric processes like the North Atlantic Oscillation (NAO), described as the major forcing behind moisture penetration, North Atlantic westerlies position and the consequent penetration of winter storm tracks into the western Mediterranean region (Hurrell 1995; Trigo et al. 2004), has been suggested as millennial-scale phenomenon controlling the ~1500 year cycle (Thompson and Wallace 2001; Debret et al. 2007). Recently, this cycle has also been interpreted as a high frequency extension of the Milankovitch precessional cycles, incorporating orbital, solar and lunar forcing through interaction with the tropical and anomalistic years and the Earth's rotation (Kelsey et al. 2015). Thus, a single theory explaining the formation of this cycle does not exist, and it is interpreted as caused by a combination of several

forcing mechanisms (Wanner and Bütikofer 2008; Wanner et al. 2011, 2015; Smith et al. 2016, and references therein).

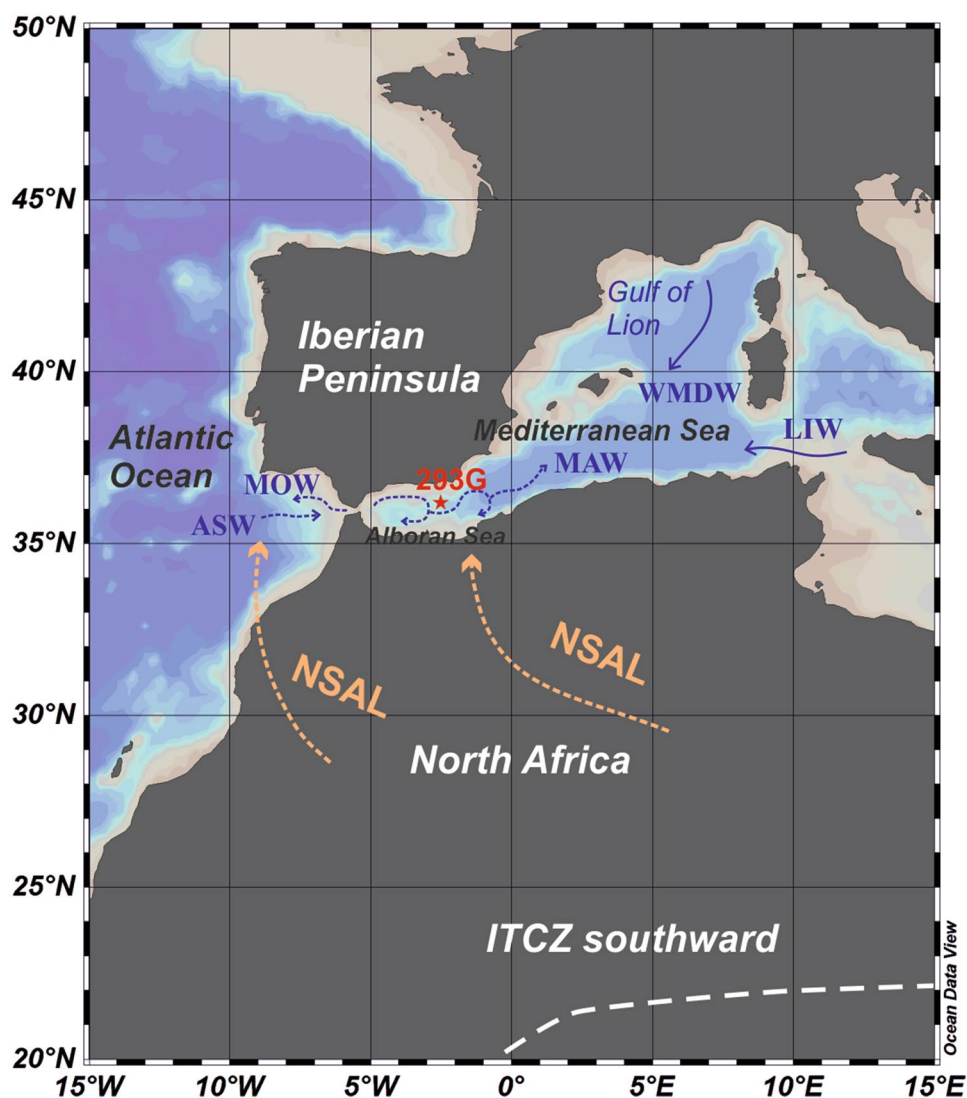
Previous spectral analysis based on the Lomb–Scargle method on time series from the westernmost Mediterranean Sea (Alboran Sea basin) has revealed four significant climate cycles over the last 20 kyr, including the 1500 year cycle, which was interpreted as related to the coupling of North Atlantic climate variability and the African monsoon system (Rodrigo-Gámiz et al. 2014a). However, the response of different paleoclimate proxies to the forcing and the phase relationships between the different responses of the climate system relatives to this cycle have been less investigated. Here we present further detailed cross-spectral analysis performed on existing high-resolution paleoenvironmental data sets in order to evaluate leads or lags in the 1500 year climate cycle. This analysis provides further insights into the incidence of the Bond cycle and time shifts of the different components of the climate system to the forcing, highlighting the complex interaction between ocean and atmosphere responses to forcing mechanisms in the westernmost Mediterranean.

### 1.1 Present climate and oceanographic conditions in the western Mediterranean

The Alboran Sea basin is located in the westernmost Mediterranean Sea, SE of Iberia and NW of North Africa (Fig. 1). This basin presents exceptional high sedimentation rates, where terrigenous sediments are mainly supplied by riverine discharge from the southern Iberian rivers, and by eolian dust pulses from Morocco, Mauritania, Mali, Niger and Algeria (Martínez Ruiz et al. 2015; Rodrigo-Gámiz et al. 2015a).

The present-day climate in this area is characterized by a strong seasonal contrast, featuring hot, dry summers and humid, mild winters (Lionello et al. 2006). At the decadal scale, climate is strongly influenced by the North Atlantic Oscillation (NAO), governed by the difference between surface sea-level pressure of the subpolar Icelandic cyclone and the subtropical Azores anticyclone (Trigo et al. 2004). An intensified Azores anticyclone and a deeper Icelandic cyclone, translated as a positive NAO phase, generate the northward migration of the Atlantic westerly jet, leading to wetter and warmer winter conditions in northwestern Europe and drier conditions in the southern Mediterranean. Conversely, during a negative NAO phase, the Azores anticyclone is weaker and the Icelandic cyclone shallower, resulting in humid westerlies in the southern Mediterranean and increased precipitation (Wanner et al. 2001). In addition to exerting inter-annual control over the European climate, NAO-like conditions are thought to persist over longer centennial timescales, due to a relatively stable

**Fig. 1** Location of marine sediment record 293G studied in the Alboran Sea basin. *Blue dashed arrows* represent theoretical surface sea water circulation in the westernmost Mediterranean, i.e. the influx of Atlantic Surface Water (ASW), the circulation of Modified Atlantic Water (MAW) in the Alboran Sea, and the Mediterranean Outflow Waters (MOW) to the Atlantic Ocean. *Blue arrows* represent deeper sea water masses, Western Mediterranean Deep Water (WMDW) formation in the Gulf of Lion, and Levantine Intermediate Water (LIW). *Orange dashed arrows* indicate theoretical wind trajectories of the northern branch of Saharan Air Layers (NSAL) over North Africa. The *white dashed line* shows the southward position of the Inter-Tropical Convergence Zone (ITCZ). Map designed with Ocean Data View application, ODV4 Release 4.7.9. (Schlitzer R, Ocean Data View, <http://odv.awi.de>, 2017)



positioning of the westerlies during periods of the Holocene (Olsen et al. 2012).

The climate conditions are also modulated by the Inter-Tropical Convergence Zone (ITCZ) over North Africa and the variability of the west African monsoon rainfall (Nicholson 2009). The ITCZ is the system where the moisture available for convection is strongly coupled to the strength of the uplift, which in turn is controlled by the characteristics of the African Easterly Jet–African Easterly Wave system (AEJ–AEW) (Cornforth et al. 2009). The AEJ–AEW system is developed over northern Africa during the boreal summer season (Mekonnen et al. 2006). During boreal summer, the dry subtropical air shifts northward and the ITCZ is located around 20°N, marking the onset of the rainy season (summer monsoon) in North Africa—that is, heavy rainfall and higher river runoff. Conversely, in winter, the equator-ward displacement of the ITCZ (10°N) causes a southward shift of dry subtropical air masses. The

Saharan air layer (SAL) and its northern branch (NSAL) are the wind systems that allow propagating dust transport over the tropical Atlantic and the Mediterranean through the atmosphere depending on the vertical extent of the dust layer and the upper level winds. Thus perturbations in SAL significantly interact with regional climate variability through the AEJ–AEW system (Zipser et al. 2009). AEWs have also been found to play a role in mobilizing and transporting Saharan dust within Africa and globally (Jones et al. 2003; Knippertz and Todd 2010). Enhanced (suppressed) dust in NSAL are significantly correlated to robust mid-level dipole vorticity disturbances downstream of the AEJ core, along with strengthened (weakened) correlative low-level trade winds in northern and southern edges of the Atlantic ITCZ (Hosseinpour and Wilcox 2013).

From an oceanographic standpoint, the western Mediterranean Sea is characterized by a thermohaline circulation driven by excessive evaporation with respect to

precipitation and runoff (e.g. Béthoux 1979). Hence, the Atlantic jet stream becomes saltier and denser when it flows into the Mediterranean Sea (modified Atlantic water, MAW), and two anticyclonic gyres are produced when it progresses eastward to the Algerian Basin (Western and Eastern Alboran Gyres) (Millot 1999). The MAW is offset by a deep-water outflow (Mediterranean Outflow Water; MOW) consisting of Levantine Intermediate Water (LIW) and Western Mediterranean Deep Water (WMDW), respectively originated in the Levantine Mediterranean Sea and in the Gulf of Lion (e.g. Millot 2008).

## 2 Data sets and cross-spectral analysis

The data sets used for this study derive from a selected sediment record, core 293G, recovered in the East Alboran Sea basin (Fig. 1) (lat. 36°10.414N, long. 2°45.280W, depth 1840 m), during the oceanographic cruise Training Through Research-12 (Comas and Ivanov 2003). The entire record of 402 cm length was sampled at very high-resolution, each 1.5 cm, obtaining a total of 267 samples. Previous data obtained from this sediment record provided new insights into the paleoclimate and paleoceanographic responses in the westernmost Mediterranean over the last 20 kyr (Rodrigo-Gámiz et al. 2011, 2014b, 2015a). Moreover, the cyclostratigraphic analysis of the existing data sets ( $N=267$  samples with a temporal resolution of ca. 75 years) has shown four main climate periodicities evidenced by selected paleoenvironmental proxies (terrigenous input, redox conditions, productivity, temperature and salinity), also allowing for the identification of climate cycles and forcing mechanisms during this time period (Rodrigo-Gámiz et al. 2014a).

### 2.1 Paleoenvironmental proxies

The selected detrital proxies used, the K/Al and Zr/Al ratios, are related to different sediment transport mechanisms, respectively fluvial runoff and eolian input (e.g. Calvert and Pedersen 2007). Bottom water oxygen conditions are revealed by redox sensitive element ratios such as the V/Al and U/Th ratios, widely used in the Mediterranean for paleoenvironmental reconstructions (e.g. Martínez-Ruiz et al. 2015, and references therein). In particular, V is reduced to an insoluble species of lower valence under anoxic conditions, while U may also form a complex with dissolved fulvic acid in hemipelagic sediments (e.g. Calvert and Pedersen 2007, and references therein). Marine productivity variations are indicated by the Ba/Al ratio, since Ba excess derives from marine barite accumulated during high productivity periods (e.g. Griffith and Paytan 2012). Sea surface temperature and salinity variations have been

reconstructed from an organic proxy, in particular the  $U^{K'}_{37}$  index (Prahl and Wakeham 1987), and oxygen stable isotopes composition (Urey 1947; Fischer and Wefer 1999), whereas further salinity calculations have been obtained using the equation proposed by Rostek et al. (1993).

### 2.2 Cross-spectral analysis

Cross-spectral analysis allows hidden relationships between pairs of variables in the spectral domain to be discovered (Chatfield 1991). It should be noted that the classic cross-spectral analysis, applied here, assumes that the relations between variables are linear. Although there are different methodologies for direct spectral analysis, not all of them can be adapted to cross-spectral analysis, a problem further complicated by the fact that most time series in cyclostratigraphy have an uneven sampling. For instance, even when sampling is continuous along a borehole core, the transformation to a time scale using different datings would produce an uneven time series because the sedimentation rates are rarely constant over long periods. Thus, one versatile possibility is to use the Lomb-Scargle periodogram (Lomb 1976; Scargle 1982; Press et al. 1992) extended to perform cross-spectral analysis using the CSLOMBS program (cross-periodogram, squared coherence and phase), which lies in the evaluation of the statistical significance of the peaks by the permutation test (Pardo-Igúzquiza and Rodríguez-Tovar 2012; Pardo-Igúzquiza et al. 2014). In the realm of cyclostratigraphy, the most interesting functions of cross-spectral analysis are the cross-spectrum, the squared coherence spectrum and the phase spectrum (Weedom 2003). Our approach to cross-spectral analysis does not stem from the cross-covariance function but rather from smoothing the cross-periodogram [see first and second approaches in Chatfield (1991)]. The statistical significance of the cross-spectral analysis is calculated by means of the permutation test, a non-parametric method described by Pardo-Igúzquiza and Rodríguez-Tovar (2000, 2005).

In the case of two or more time series, cross-spectral analysis may reveal the correlation of each pair of time series in the frequency domain. In this study, we work with eight different data sets with uneven sampling but from the same time series, i.e. each data set has  $N$  experimental data (up to  $N=267$ ) but all were measured over the same time interval (eight paleoenvironmental proxies from a marine sediment record covering the last 20 kyr). The resolution of the sampling interval ( $N=267$  samples with a temporal resolution of ca. 75 years), can be considered good enough when working with the Lomb-Scargle periodogram analysis here conducted [see Rodrigo-Gámiz et al. (2014a) for a detailed explanation].

The results of cross-spectral analysis using the program CSLOMBS (see details in Pardo-Igúzquiza and

Rodríguez-Tovar 2012) and the statistical significance for each pair of time series are displayed in three profiles: (a) the squared coherence spectrum with the frequency cycles obtained; (b) the achieved confidence level, or coherence (in %) for the 1400 year cycle; and (c) the phase spectrum in degree, which shows in phase ( $0^\circ$  and  $360^\circ$ ), out of phase ( $180^\circ$ ) or intermediate phase ( $90^\circ$  and  $270^\circ$ ).

In addition, phase relationships for the data sets in degrees—i.e. leads ( $0$ – $180^\circ$ ) and lags ( $0$  to  $-180^\circ$ ), or the equivalent time shifts in years—are illustrated in phase wheel diagrams (Weedom 2003). The vector angle represents in phase to intermediate leads ( $0$  to  $90^\circ$ ) or lags ( $0$  to  $-90^\circ$ ) and the intermediate to out of phase leads ( $90^\circ$  to  $180^\circ$ ) or lags ( $-90^\circ$  to  $-180^\circ$ ).

### 3 Results

Obtained results are illustrated in Fig. 2, showing the squared coherence spectrum with the frequency cycles, the achieved confidence level, and the phase spectrum.

According with the squared coherence spectrum between the pair of time series K/Al and Ba/Al ratios from marine record 293G shows frequency cycles at 2.7 kyr, 1.4 kyr, 442 yr and 373 yr (Fig. 2a). The coherence of the 1.4 kyr cycle is very high, giving a confidence level over 95% (Fig. 2b), and the phase spectrum is out of phase with an angle of  $112^\circ$  (Fig. 2c). This cycle, associated with the Bond cycle, is considered equivalent to the 1515 yr cycle described in Rodrigo-Gámiz et al. (2014a) due to the uncertainty is of the order of 100 years, similar to the sampling interval (75 years).

The cross-spectral analysis profiles for each pair of time series from marine record 293G are shown in the Supplementary Material. Non-correlation was obtained in the cross-spectral analysis of the  $\delta^{18}\text{O}$  signal with any of the other proxies used.

Each angle implies a time lead or lag for the 1.4 kyr cycle that is represented in the phase wheels (Fig. 3) and as summary in Table 1. Note that the possible uncertainty is marked with colour shaded areas in Fig. 3, approximating the value obtained to the nearest, i.e. to  $\frac{1}{4}$  of phase (close to  $90^\circ$  equivalent to 350 year), to out of phase (close to  $180^\circ$  equivalent to 700 year), or to  $\frac{3}{4}$  of phase (close to  $135^\circ$  equivalent to 525 year).

The K/Al–U/Th and K/Al–Ba/Al relationships present an angle of  $101^\circ$ – $112^\circ$ , respectively, which imply a time leads of 350–436 year (Fig. 3a). The K/Al vs Zr/Al ratios are also out of phase with an angle of  $138^\circ$  or time shift of 537 year (Fig. 3a). The K/Al ratio vs both  $U^{K'}_{37}$  and salinity present respective angles of  $170^\circ$  and  $168^\circ$ , meaning time leads of ca. 700 year (661 and 653 year, respectively) (Fig. 3a).

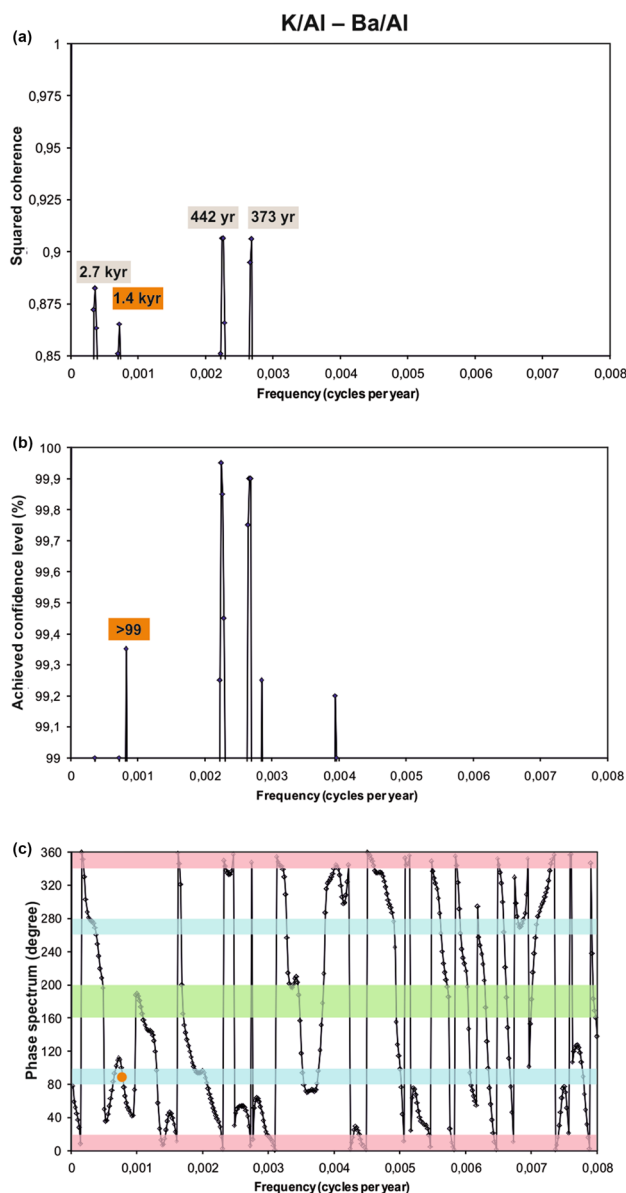


**Fig. 2** a Squared coherence cross-spectrum between the pair time series K/Al–Ba/Al from marine record 293G showing the cross-spectral peaks obtained; b achieved confidence level (ACL, %); and c phase spectrum (degree), where red bands show the phase spectrum, blue bands show the intermediate phase, and the green band shows out of phase. The Bond cycle is colored in orange

The V/Al ratio and  $U^{K'}_{37}$  present an angle of  $101^\circ$  or time shift of 350–392 year, meanwhile V/Al ratio and Salinity are almost completely out of phase, with an angle of  $175^\circ$  and consequently a time lead of 681–700 year (Fig. 3b).

In turn, the U/Th ratio and  $U^{K'}_{37}$  show an angle of  $119^\circ$  or a time shift of 350–430 year when translated to a time lead (Fig. 3c).

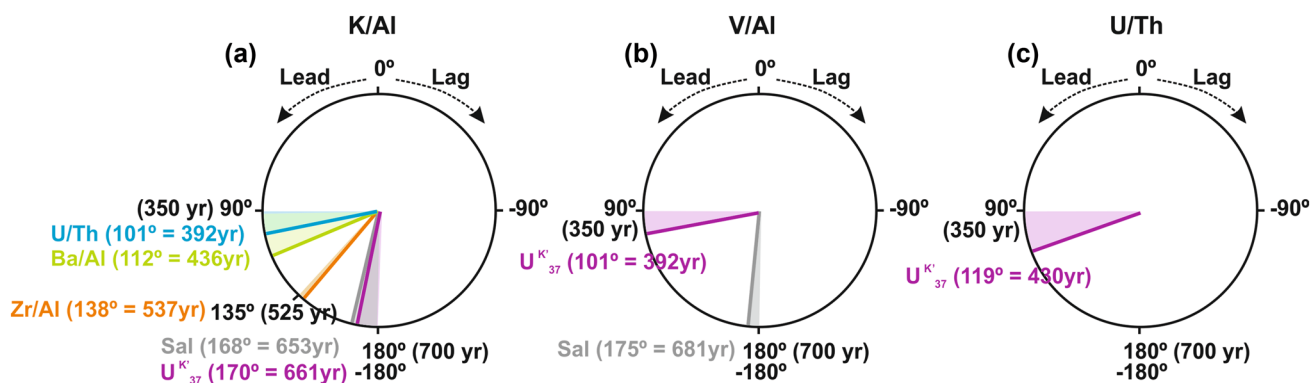


**Fig. 3** Cross-spectral phase wheels of the pairs of paleoenvironmental proxies with very high correlation (>95% ACL) for the last 20 kyr. Vector angle represents intermediate to phase (0 to 90°) and intermediate to out of phase (90° to 180°). Numerical values next to each proxy show the time leads in years (yr) equivalent to each angle. Colour shaded areas show the range of uncertainty considered. Due to the time series are very short, the value is approximated to the near-

est, i.e. to  $\frac{1}{4}$  of phase (close to 90° equivalent to 350 year), to out of phase (close to 180° equivalent to 700 year), or to  $\frac{3}{4}$  of phase (close to 135° equivalent to 525 year). Detrital proxies (Zr, K) are in orange, oxygenation proxies (V, U) are in blue, productivity proxy (Ba) is in green, temperature proxies ( $U^{K}_{37}$ ,  $\delta^{18}O$ ) are in purple, and salinity proxy (Sal) is in gray

**Table 1** Climate significance of the different paleoenvironmental proxies analyzed and time lead (in years) obtained

Paleoenvironmental proxy	Provenance	Climate significance	Lead (years)
K/Al	Illite	Detrital component, fluvial input	Reference
Zr/Al	Zircon	Detrital component, eolian input	537
V/Al	Trace element in sediment	Bottom water oxygen conditions	–
U/Th	Trace element in sediment	Bottom water oxygen conditions	392
Ba/Al	Detrital/biogenic barite	Paleoproductivity	436
$\delta^{18}O$	Planktonic forams	Temperature and salinity	–
Salinity	Planktonic forams/Haptophyte	Salinity	653
$U^{K}_{37}$	Haptophyte algae	Temperature	661

## 4 Discussion

The Bond climate cycle has been previously evidenced in the western Mediterranean during the last 20 kyr through a rapid response in both oceanic and atmospheric systems, as indicated by diverse geochemical ratios (Rodrigo-Gámiz et al. 2014a). Typical fluvially derived proxies, certain eolian input proxies, redox and productivity proxies showed this periodicity at very high (>95%) confidence level, but with no significance in the  $\delta^{18}O$  signal, used as the paleotemperature–paleosalinity proxy (Rodrigo-Gámiz et al. 2014a). This short-term periodicity has also been recorded in other western Mediterranean records during the last glacial cycle and the Holocene by proxies such as the Si/(Si + K) ratio as indicator of eolian input and wind intensity (Moreno et al. 2005), the  $\delta^{18}O$  in foraminifera (Sierro et al. 2005), changes in thermohaline circulation (Cacho et al. 1999, 2000; Martrat et al. 2007), and Mediterranean vegetation variations (Fletcher et al. 2013).

The lead–lag relationships between diverse paleoenvironmental proxies have not been previously investigated, however this analysis makes possible to evaluate the time response of the different components of the climate system to the Bond cycle. Thus, the cross-spectral analysis performed here on the existing data sets provides additional information about the time shifts for each paleoenvironmental response to the input of the Bond climate cycle. Out of phase (non-correlation) relationships were obtained in the cross-spectral analysis of the  $\delta^{18}O$  signal with any of the other proxies used. The planktic foraminifera  $\delta^{18}O$  signal integrates a more local signal, not only involving the global ice volume and temperature, but also local changes in the hydrological cycle. Recent models simulating local salinity and  $\delta^{18}O$  (relative to  $^{18}O$  abundance in sea water) for the glacial-interglacial cycles show that variations are not coeval, and the relationship is not maintained over time (Ganopolski and Roche 2009).

Taking as reference the terrigenous fluvial input proxy determined by the K/Al ratio, all the other

paleoenvironmental proxies were out of phase, showing different time shifts or leads–lags, driving one change that prevailed over others (Fig. 3; Table 1). The first lead was shown by the SST proxy  $U^{K'}_{37}$ , and salinity, indicating the highest time shift, ca. 700 year (661–653 year) (Fig. 3a). It supports an initial oceanic response to the Bond cycle in the western Mediterranean with the inflow of cold and less salty Atlantic waters (Fig. 4). This finding would be in agreement with the nature of this climate cycle, described as the penetration of cold surface waters into the North Atlantic driving changes in the North Atlantic thermohaline circulation (Bond et al. 1993, 2001; Broecker 1994). Previous wavelet analysis performed in paleorecords from Atlantic, Mediterranean, Pacific and circum-Antarctic regions spanning the Holocene also evidenced that the 1500 year climate cycle may be associated with oceanic internal forcing, and not only with changes in the sun's intensity (Debret et al. 2007, 2009; Denton and Broecker 2008; Sorrel et al. 2012), possibly representing a threshold response in North Atlantic Ocean circulation to external solar cycles (Dima and Lohmann 2009).

The interplay between Atlantic and Mediterranean water mass circulation is essential for a better understanding of the evolution of the Modified Atlantic Water (MAW) from the Atlantic to the Mediterranean and the Mediterranean Outflow Water (MOW) from the Mediterranean towards the Atlantic, playing a major role in North Atlantic circulation resumption (Voelker et al. 2006). Under an inflow of cold North Atlantic waters into the westernmost Mediterranean, towards a dominant positive NAO mode and a southward position of the ITCZ, progressively more arid conditions in the area showed a lead of ca. 525 year (537 year) (Fig. 3a), noted by the eolian input proxy  $Zr/Al$  ratio (Fig. 4). The  $Zr/Al$  signal, which is related to heavy minerals transported

by intense winds, indicates an atmospheric intensification of the northern branch of Saharan Air Layers (NSAL) or the African Easterly Jet–African Easterly Wave system (AEJ–AEW) over the arid Sahara region (Zipser et al. 2009; Knippertz and Todd 2010), transporting eolian dust to the western Mediterranean (Fig. 4).

Eolian dust input transported by trade winds from northwestern Africa has been previously linked with the 1500 year cycle (deMenocal and Rind 1993), apparently modulated by a positive NAO mode (Trigo et al. 2004) generating dry and cold conditions over southern Europe. NAO-like mechanisms have likewise been invoked to explain SST-cooling events recorded in the western Mediterranean (Cacho et al. 1999). The ITCZ migrations over North Africa involve detrital input variations into the western Mediterranean basin, shown by climate models (Lee et al. 2011), where dry conditions and eolian dust pulses in North Africa are triggered by the southward migration of the ITCZ and the AEJ-AEW system (Cornforth et al. 2009). These atmospheric variations would have occurred after the SST-cooling of the surface waters (Fig. 4). Nevertheless, feedbacks between changes in insolation and oceanic–atmospheric circulations have also explained fluctuations in the West African monsoon (Gasse 2000).

Later on, changes in the Mediterranean thermohaline circulation, noted by the U/Th ratio, showed a time shift of 392 year (ca. 350 year) (Fig. 3a). Furthermore, SST led both redox proxies, V/Al and U/Th ratios, with a time shift of ca. 350 year (Fig. 3b, c), while salinity showed a lead of ca. 700 year with V/Al ratio (Fig. 3b). Nevertheless, the dynamical response of both SST and salinity led changes in oxygen concentration in the sediment or water column, pointing out that the internal oceanic response had a more complex evolution than a simple linear response.

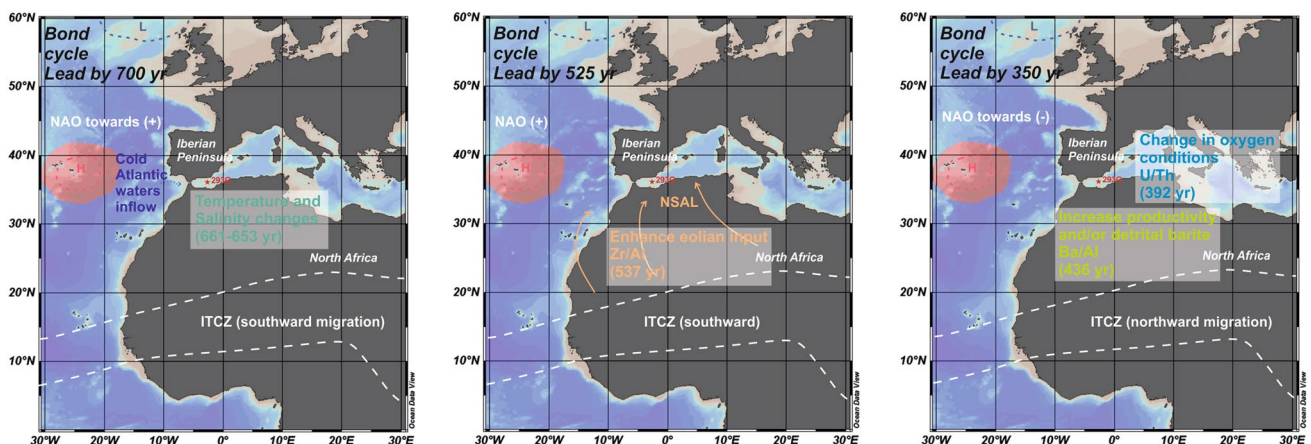


**Fig. 4** Schematic map of the western Mediterranean with the dynamical response and time lead in years, considering as reference the  $K/Al$  ratio (fluvial input proxy), of the different paleoenvironmental

proxies used in the cross-spectral analysis for the last 20 kyr. Map designed with Ocean Data View application, ODV4 Release 4.7.9. (Schlitzer R, Ocean Data View, <http://odv.awi.de>, 2017)

Following both oceanic and atmospheric responses, the Ba enrichments indicated by the Ba/Al ratio lead the fluvial response by ca. 350 year (436 year) (Figs. 3a, 4). Although both authigenic and detrital barite may have contributed to enhanced Ba concentration in the Alboran Sea sediment records, variations in Ba profiles seem to be related to productivity oscillations associated with a greater supply of nutrients, also linked to variations in the wind systems over the western Mediterranean (Bassetti et al. 2010). Still, the biogeochemistry of Ba is not fully understood in the westernmost Mediterranean and further studies are required. During the last two millennia, the Ba contents appear to be associated with a detrital origin, fluvially derived, and linked to alumino-silicates (Nieto-Moreno et al. 2011). In contrast, the significant Ba enrichments during cold and arid periods such as the Younger Dryas and the last Heinrich event would also suggest an important contribution from productivity (Rodrigo-Gámiz et al. 2011). Furthermore, productivity changes with a near 1500 year periodicity has been documented in a marine record spanning the last 15 kyr from the Sicily Channel (Incarbona et al. 2008), reporting oceanic and atmospheric circulation variability with consequent relocation of the nutricline within the photic zone as one of the most important forcing mechanism for Holocene coolings in the Mediterranean. An intensification of the NSAL or the AEJ–AEW system and dust transport to the western Mediterranean could have triggered a biological response with an increase of productivity as showed the lead in the Ba/Al ratio (Fig. 4). Nevertheless, a detailed study of the barite minerals would be required to elucidate the provenance of Ba in this area over the last 20 kyr.

A progressively change in the NAO mode (towards negative), a northward migration in the ITZC with an increase of the monsoon activity, or just sporadic rainfalls in the western Mediterranean area, would results in a final enhance of humidity and runoff with a latest fluvial response represented by the K/Al ratio (Fig. 4). Phases of high storm activity during the Late Holocene in cold periods at the ~1500 year cycles of IRD have also been documented in the northwestern Mediterranean (Degeai et al. 2015), thus evidencing the oceanic and atmospheric teleconnection between Atlantic and Mediterranean climate variability.

In sum, the variety of paleoenvironmental proxies used in this study evidence different time shifts leading the Bond cycle, supporting a first oceanic response to this cycle followed by its interplay with the atmospheric response, linked to changes in the Atlantic circulation, the meridional atmospheric variability and the West African monsoon system, and the NAO indices as have been previously documented (e.g. Tuenter et al. 2007; Scheinwald and Billups 2012).

## 5 Conclusions

Previous cyclostratigraphic studies on a marine sediment record (293G) from the western Mediterranean spanning the last 20 kyr have evidenced four main climate cycles, including the Bond cycle, in terrigenous, redox and productivity, sea surface temperature (SST) and salinity proxies. A new cross-spectral analysis of these existing paleoenvironmental time series reveals the time shift response of the different components of the climate system to the input of the 1400 year cycle. Considering as reference the terrigenous fluvial input proxy determined by the K/Al ratio, all the other paleoenvironmental proxies were out of phase. The first time leads were shown by  $U^{K'_{37}}$ , as SST proxy, and salinity, with a time shift of ca. 700 year (661–653 year). Then the Zr/Al ratio, as the eolian input proxy, leads by ca. 525 year (537 year). The U/Th ratio showed a time shift of 392 year (ca. 350 year). In addition, SST and salinity led changes in redox proxies, both V/Al and U/Th ratios, showing leads of ca. 350 year (392 and 430 year respectively), evidencing a more complex oceanic evolution with changes in the Mediterranean thermohaline circulation. Following the oceanic and atmospheric responses, the enrichments in Ba, indicated by the Ba/Al ratio, also lead ca. 350 year (436 year), although both authigenic and detrital barite may have contributed to enhanced Ba concentrations. These results suggest a prior oceanic response to the Bond cycle in the western Mediterranean tied to changes of the NAO mode, and the ITCZ with variations in the African monsoon activity and the Saharan winds system, with a complex relationship between the involved phenomena.

**Acknowledgements** This study was supported by the European Regional Development Fund (ERDF)-cofinanced Grants CGL2015-66835-P, CGL2015-66830-R, and CGL2015-71510-R (Secretaría de Estado de Investigación MINECO), Research Groups RNM 179, RNM 178 (Junta de Andalucía), and the Research Excellence Unit (UCE-PP2016-05) of the University of Granada. We are also grateful to the oceanographic cruise Training-Through-Research Programme (UNESCO-Moscow State University). M. Rodrigo-Gámiz acknowledges funding from “Ayudas para el mantenimiento de la actividad de los grupos de investigación de la UGR” within the program “Fortalecimiento de las capacidades de I+D+I” from the University of Granada, and from the Andalucía Talent Hub Program co-funded by the European Union’s Seventh Framework Program (COFUND—Grant Agreement No 291780) and the Junta de Andalucía. We thank the Editor J.-C. Duplessy and three anonymous reviewers for their constructive comments.

## References

- Alley RB, Brook EJ, Anandkrishnan S (2002) A northern lead in the orbital band: north–south phasing of Ice-Age events. *Quat Sci Rev* 21:431–441

- Bassetti M-A, Carbonel P, Sierro FJ, Perez-Folgado M, Jouët G, Berné S (2010) Response of ostracods to abrupt climate changes in the Western Mediterranean (Gulf of Lion) during the last 30 kyr. *Mar Micropaleontol* 77:1–14. doi:[10.1016/j.marmicro.2010.06.004](https://doi.org/10.1016/j.marmicro.2010.06.004)
- Béthoux JP (1979) Budgets of the Mediterranean Sea. Their dependence on the local climate and on the characteristics of the Atlantic waters. *Oceanol Acta* 2:157–163
- Bond G, Broecker WS, Johnsen SJ, McManus J, Labeyrie L, Jouzel J, Bonani G (1993) Correlations between climate records from North Atlantic sediments and Greenland ice. *Nature* 365:143–147
- Bond G, Showers W, Cheseby M, Lotti R, Almasi P, deMenocal P, Priore P, Cullen H, Hajdas I, Bonani G (1997) A pervasive millennial-scale cycle in North Atlantic Holocene and Glacial climates. *Science* 278:1257–1266
- Bond G, Kromer B, Beer J, Muscheler R, Evans MN, Showers W, Hoffmann S, Lotti-Bond R, Hajdas I, Bonani G (2001) Persistent solar influence on North Atlantic climate during the Holocene. *Science* 294:2130–2135. doi:[10.1126/science.1065680](https://doi.org/10.1126/science.1065680)
- Broecker WS (1994) Massive iceberg discharges as triggers for global climate change. *Nature* 372:421–424
- Broecker WS (1997) Paleocean circulation during the last deglaciation; a bipolar seesaw? *Paleoceanography* 13:119–121
- Cacho I, Grimalt JO, Pelejero C, Canals M, Sierro FJ, Flores JA, Shackleton NJ (1999) Dansgaard-Oeschger and Heinrich event imprints in the Alboran Sea paleotemperatures. *Paleoceanography* 14:698–705
- Cacho I, Grimalt JO, Sierro FJ, Shackleton NJ, Canals M (2000) Evidences for enhanced Mediterranean thermohaline circulation during rapid climatic coolings. *Earth Planet Sci Lett* 183:417–429. doi:[10.1016/S0012-821X\(00\)00296-X](https://doi.org/10.1016/S0012-821X(00)00296-X)
- Calvert SE, Pedersen TF (2007) Chapter fourteen elemental proxies for palaeoclimatic and palaeoceanographic variability in marine sediments: interpretation and application. In: Hillaire-Marcel C, De Vernal A (eds) *Proxies in Late Cenozoic Paleooceanography, developments in marine geology*. Elsevier, Oxford, pp 567–644
- Chatfield C (1991) *The analysis of time series: an introduction*, 4th edn. Chapman and Hall, London
- Comas MC, Ivanov MK (2003) Alboran basin (Leg 3). In: Kenyon H, Ivanov MK, Akhmetzhanov AM, Akhmanov GG (eds) *Interdisciplinary geoscience research on the North East Atlantic margin, Mediterranean Sea and Mid-Atlantic Ridge*. Technical Series UNESCO, pp 51–71
- Cornforth RJ, Hoskins BJ, Thorncroft CD (2009) The impact of moist processes on the African Easterly Jet–African Easterly Wave system. *Q J R Meteorol Soc* 135:894–913
- Debret M, Bout-Roumzeilles V, Grousset F, Desmet M, McManus JF, Massei N, Sebag D, Petit JR, Copard Y, Trentesaux A (2007) The origin of the 1500-year climate cycles in Holocene north-atlantic records. *Clim Past* 3:569–575. doi:[10.5194/cp-3-569-2007](https://doi.org/10.5194/cp-3-569-2007)
- Debret M, Sebag D, Crosta X, Massei N, Petit JR, Chapron E, Bout-Roumzeilles V (2009) Evidence from wavelet analysis for a mid-Holocene transition in global climate forcing. *Quat Sci Rev* 28:2675–2688. doi:[10.1016/j.quascirev.2009.06.005](https://doi.org/10.1016/j.quascirev.2009.06.005)
- Degeai JP, Devillers B, Dezileau L, Oueslati H, Bony G (2015) Major storm periods and climate forcing in the Western Mediterranean during the Late Holocene. *Quat Sci Rev* 129:37–56. doi:[10.1016/j.quascirev.2015.10.009](https://doi.org/10.1016/j.quascirev.2015.10.009)
- deMenocal PB, Rind D (1993) Sensitivity of Asian and African climate to variations in seasonal insolation, glacial ice cover, sea surface temperatures, and Asian orography. *J Geophys Res* 98:7265–7287
- Denton GH, Broecker WS (2008) Wobbly ocean conveyor circulation during the Holocene?. *Quat Sci Rev* 27:1939–1950. doi:[10.1016/j.quascirev.2008.08.008](https://doi.org/10.1016/j.quascirev.2008.08.008)
- Dima M, Lohmann G (2009) Conceptual model for millennial climate variability: a possible combined solar-thermohaline circulation origin for the 1,500-year cycle. *Clim Dyn* 32:301–311. doi:[10.1007/s00382-008-0471-x](https://doi.org/10.1007/s00382-008-0471-x)
- Fischer G, Wefer G (1999) *Use of proxies in paleoceanography: examples from the South Atlantic*. Springer, Berlin
- Fletcher WJ, Debret M, Sanchez Goñi MF (2013) Mid-Holocene emergence of a low-frequency millennial oscillation in western Mediterranean climate: implications for past dynamics of the North Atlantic atmospheric westerlies. *The Holocene* 23:153–166. doi:[10.1177/0959683612460783](https://doi.org/10.1177/0959683612460783)
- Ganopolski A, Roche DM (2009) On the nature of lead-lag relationships during glacial interglacial climate transitions. *Quaternary Sci Rev* 28:3361–3378. doi:[10.1016/j.quascirev.2009.09.019](https://doi.org/10.1016/j.quascirev.2009.09.019)
- Gasse F (2000) Hydrological changes in the African tropics since the last glacial maximum. *Quat Sci Rev* 19:189–211. doi:[10.1016/S0277-3791\(99\)00061-X](https://doi.org/10.1016/S0277-3791(99)00061-X)
- Griffith EM, Paytan A (2012) Barite in the ocean—occurrence, geochemistry and palaeoceanographic applications. *Sedimentology* 59:1817–1835. doi:[10.1111/j.1365-3091.2012.01327.x](https://doi.org/10.1111/j.1365-3091.2012.01327.x)
- Hosseinpour F, Wilcox E (2013) Interactions between Oceanic Saharan air layer and African Easterly Jet–African Easterly waves system. American Geophysical Union, Fall Meeting, abstract GC13A-1058.
- Hurrell JW (1995) Decadal trends in the North Atlantic Oscillation: regional temperatures and precipitation. *Science* 269:676–679. doi:[10.1126/science.269.5224.676](https://doi.org/10.1126/science.269.5224.676)
- Incarbona A, Di Stefano E, Patti B, Pelosi N, Bonomo S, Mazzola S, Sprovieri R, Tranchida G, Zgozi S, Bonanno A (2008) Holocene millennial-scale productivity variations in the Sicily Channel (Mediterranean Sea). *Paleoceanography* 23:PA3204. doi:[10.1029/2007PA001581](https://doi.org/10.1029/2007PA001581)
- Jones C, Mahowald N, Luo C (2003) The role of easterly waves on African desert dust transport. *J Clim* 16:3617–3628
- Kelsey AM, Menk FW, Moss PT (2015) An astronomical correspondence to the 1470 year cycle of abrupt climate change. *Clim Past Discuss* 11:4895–4915. doi:[10.5194/cpd-11-4895-2015](https://doi.org/10.5194/cpd-11-4895-2015)
- Knippertz P, Todd MC (2010) The central west Saharan dust hot spot and its relation to African easterly waves and extratropical disturbances. *J Geophys Res* 115:D12117
- Lee S-Y, Chiang JCH, Matsumoto K, Tokos KS (2011) Southern Ocean wind response to North Atlantic cooling and the rise in atmospheric CO<sub>2</sub>: modeling perspective and paleoceanographic implications. *Paleoceanography* 26:PA1214. doi:[10.1029/2010PA002004](https://doi.org/10.1029/2010PA002004)
- Lionello P, Malanotte-Rizzoli P, Boscolo R, Alpert P, Artale V, Li L, Luterbacher J, May W, Trigo R, Tsimplis M, Ulbrich U, Xoplaki E (2006) The Mediterranean climate: an overview of the main characteristics and issues. In: Lionello P, Malanotte-Rizzoli P, Boscolo R (eds) *Mediterranean climate variability, developments in earth and environmental sciences*. Elsevier, Amsterdam, pp 1–26
- Lomb NR (1976) Least-squares frequency analysis of unequally spaced data. *Astrophys Space Sci* 39:447–462
- Martínez-Ruiz F, Kastner M, Gallego-Torres D, Rodrigo-Gámiz M, Nieto-Moreno V, Ortega-Huertas M (2015) Paleoclimate and paleoceanography over the last 20,000 year in the Mediterranean Sea Basins as indicated by sediment elemental proxies. *Quat Sci Rev* 107:25–46. doi:[10.1016/j.quascirev.2014.09.018](https://doi.org/10.1016/j.quascirev.2014.09.018)
- Martrat B, Grimalt JO, Shackleton NJ, de Abreu L, Hutterli MA, Stocker TF (2007) Four climate cycles of recurring deep and surfacewater destabilizations on the Iberian Margin. *Science* 317:502–507. doi:[10.1126/science.1139994](https://doi.org/10.1126/science.1139994)

- Mekonnen A, Thorncroft CD, Aiyyer AR (2006) Analysis of convection and its association with African easterly waves. *J Clim* 19:5405–5421
- Millot C (1999) Circulation in the Western Mediterranean Sea. *J Mar Syst* 20:423–442
- Millot C (2008) Short-term variability of the Mediterranean in- and outflows. *Geophys Res Lett* 35:L15603. doi:10.1029/2008GL033762
- Moreno A, Cacho I, Canals M, Grimalt JO, Sánchez Goñi MF, Shackleton N, Sierro FJ (2005) Links between marine and atmospheric processes oscillating on a millennial time-scale. A multi-proxy study of the last 50,000 year from the Alboran Sea (Western Mediterranean Sea). *Quat Sci Rev* 24:1623–1636. doi:10.1016/j.quascirev.2004.06.018
- Nicholson S (2009) A revised picture of the structure of the “monsoon” and land ITCZ over West Africa. *Clim Dyn* 32:1155–1171. doi:10.1007/s00382-008-0514-3
- Nieto-Moreno V, Martínez-Ruiz F, Giral S, Jiménez-Espejo F, Gallego-Torres D, Rodrigo-Gámiz M, García-Orellana J, Ortega-Huertas M, de Lange GJ (2011) Tracking climate variability in the western Mediterranean during the Late Holocene: a multiproxy approach. *Clim Past* 7:1395–1414. doi:10.5194/cp-7-1395-2011
- Olsen J, Anderson NJ, Knudsen MF (2012) Variability of the North Atlantic oscillation over the past 5,200 years. *Nat Geosci* 5:1–14. doi:10.1038/ngeo1589
- Pardo-Igúzquiza E, Rodríguez-Tovar FJ (2000) The permutation test as a nonparametric method for testing the statistical significance of power spectrum estimation in cyclostratigraphic research. *Earth Planet Sci Lett* 181:175–189
- Pardo-Igúzquiza E, Rodríguez-Tovar FJ (2005) MAXENPER: a program for maximum entropy spectral estimation with assessment of statistical significance by the permutation test. *Comput Geosci* 31:555–567. doi:10.1016/j.cageo.2004.11.010
- Pardo-Igúzquiza E, Rodríguez-Tovar FJ (2012) Spectral and cross-spectral analysis of uneven time series with the smoothed Lomb–Scargle periodogram and Monte Carlo evaluation of statistical significance. *Comput Geosci* 49:207–216. doi:10.1016/j.cageo.2012.06.018
- Pardo-Igúzquiza E, Rodrigo-Gámiz M, Rodríguez-Tovar FJ, Martínez-Ruiz F (2014) Cross-spectral analysis of time series with uneven sampling: study of Holocene climate variability. In: Rojas Ruiz I, Ruiz Garcia G (eds) International work-conference on time series. Proceedings ITISE. Copicentro Granada SL, Granada, pp 1–6
- Pena LD, Francés G, Diz P, Esparza M, Grimalt JO, Nombela MA, Alejo I (2010) Climate fluctuations during the Holocene in NW Iberia: high and low latitude linkages. *Cont Shelf Res* 30:1487–1496. doi:10.1016/j.csr.2010.05.009
- Prahl FG, Wakeham SG (1987) Calibration of unsaturation patterns in long-chain ketone compositions for palaeotemperature assessment. *Nature* 330:367–369
- Press HW, Teukolsky SA, Vetterling WT, Flannery BP (1992) Numerical recipes in Fortran, 2nd edn. Cambridge University Press, New York
- Rodrigo-Gámiz M, Martínez-Ruiz F, Jiménez-Espejo FJ, Gallego-Torres D, Nieto-Moreno V, Romero O, Ariztegui D (2011) Impact of climate variability in the western Mediterranean during the last 20,000 years: oceanic and atmospheric responses. *Quat Sci Rev* 30:2018–2034. doi:10.1016/j.quascirev.2011.05.011
- Rodrigo-Gámiz M, Martínez-Ruiz F, Rodríguez-Tovar FJ, Jiménez-Espejo FJ, Pardo-Igúzquiza E (2014a) Millennial- to centennial-scale climate periodicities and forcing mechanisms in the western-most Mediterranean for the past 20,000 years. *Quat Res* 81:78–93. doi:10.1016/j.yqres.2013.10.009
- Rodrigo-Gámiz M, Martínez-Ruiz F, Rampen SW, Schouten S, Sinninghe Damsté JS (2014b) Sea surface temperature variations in the western Mediterranean Sea over the last 20 kyr: a dual-organic proxy ( $U^{K}_{37}$  and LDI) approach. *Paleoceanography* 29:87–98. doi:10.1002/2013PA002466
- Rodrigo-Gámiz M, Martínez-Ruiz F, Chiaradia M, Jiménez-Espejo FJ, Ariztegui D (2015a) Radiogenic isotopes for deciphering terrigenous input provenance in the western Mediterranean. *Chem Geol* 410:237–250. doi:10.1016/j.chemgeo.2015.06.004
- Rostek F, Ruhland G, Bassinot FC, Müller P, Labeyrie LD, Lancelot Y, Bard E (1993) Reconstructing sea surface temperature and salinity using  $\delta^{18}O$  and alkenone records. *Nature* 364:319–321
- Scargle JD (1982) Studies in astronomical time series analysis. II. Statistical aspects of spectral analysis of unevenly spaced data. *Astrophys J* 263:835–853
- Scheinwald A, Billups K (2012) Millennial scale climate signals in the subtropical Northwest Atlantic. AGU Fall Meeting, Abstract PP31C–2050. San Francisco
- Sierro FJ, Hodell DA, Curtis JH, Flores JA, Reguera I, Colmenero-Hidalgo E, Bárcena MA, Grimalt JO, Cacho I, Frigola J, Canals M (2005) Impact of iceberg melting on Mediterranean thermohaline circulation during Heinrich events. *Paleoceanography* 20:PA2019. doi:10.1029/2004PA001051
- Smith AC, Wynn PM, Barker PA, Leng MJ, Noble SR, Tych W (2016) North Atlantic forcing of moisture delivery to Europe throughout the Holocene. *Nat Sci Rep* 6:24745. doi:10.1038/srep24745
- Sorrel P, Debret M, Billeaud I, Jaccard SL, McManus JF, Tessier B (2012) Persistent non-solar forcing of Holocene storm dynamics in coastal sedimentary archives. *Nat Geosci* 5:892–896. doi:10.1038/ngeo161
- Steig EJ, Alley RB (2002) Phase relationships between Antarctic and Greenland climate records. *Ann Glaciol* 35:451–456
- Thompson DWJ, Wallace JM (2001) Regional climate impacts of the northern hemisphere annular mode. *Science* 293:85–89
- Trigo RM, Pozo-Vázquez D, Osborn TJ, Castro-Díez Y, Gámiz-Fortis S, Esteban-Parra MJ (2004) North Atlantic oscillation influence on precipitation, river flow and water resources in the Iberian Peninsula. *Int J Climatol* 24:925–944. doi:10.1002/joc.1048
- Tuenter E, Weber SL, Hilgen FJ, Lourens LJ (2007) Simulating sub-Milankovitch climate variations associated with vegetation dynamics. *Clim Past* 3:169–180
- Urey HC (1947) The thermodynamic properties of isotopic substances. *J Chem Soc* 1947:562–581
- Voelker AHL, Lebreiro SM, Schönfeld J, Cacho I, Erlenkeuser H, Abrantes F (2006) Mediterranean outflow strengthening during northern hemisphere coolings: a salt source for the glacial Atlantic? *Earth Planet Sci Lett* 245:39–55. doi:10.1016/j.epsl.2006.03.014
- Wanner H, Büttikofer J (2008) Holocene Bond Cycles: real or imaginary?. *Geogr Sb ČGS* 113:338–350
- Wanner H, Bronnimann S, Casty C, Gyalistras D, Luterbacher J, Schmutz C, Stephenson DB, Xoplaki E (2001) North Atlantic oscillation—concepts and studies. *Surv Geophys* 22:321–382
- Wanner H, Solomina O, Grosjean M, Ritz S, Jetel M (2011) Structure and origin of Holocene cold events. *Quat Sci Rev* 30:3109–3123. doi:10.1016/j.quascirev.2011.07.010
- Wanner H, Mercolli L, Grosjean M, Ritz SP (2015) Holocene climate variability and change: a data-based review. *J Geol Soc* 172:254–263. doi:10.1144/jgs2013-101
- Weedon GP (2003) Times-series analysis and cyclostratigraphy: examining stratigraphic records of environmental cycles. Cambridge University Press, Cambridge
- Zipsper EJ, Twohy CH, Chee Tsay S et al (2009) The Saharan air layer and the fate of African easterly waves—NASA’s AMMA field study of tropical cyclogenesis. *Bull Am Meteorol Soc* 90:1137–1156